12. Lampart P., Yershov S. Direct constrained computational fluid dynamics based optimization of three-dimensional blading for the exit stage of a large power steam turbine. *Transactions of ASME. J. Eng. for Gas Turbines and Power.* 2003. Vol. 125. No. 1. P. 385–390. https://doi.org/10.1115/1.1520157.
13. IAPWS-95. Revised Release on the IAPWS Formulation1995 for the Thermodynamic Properties of Ordinary Water Substance for General and Scientific Use. IAPWS-95: official site, 2019. URL: http://www.iapws.org.
14. Rusanow A. V., Lampart P., Pashchenko N. V., Rusanov R. A. Modelling 3D steam turbine flow using thermodynamic properties of steam IAPWS-95. *Polish Maritime Research.* 2016. Vol. 23. No. 1. P. 61–67. https://doi.org/10.1515/pomr-2016-0009.
15. Yershov S., Rusanov A., Gardzilewicz A., Lampart P. Calculations of 3D viscous compressible turbomachinery flows. *Proc. 2nd Symp. on Comp. Technologies for Fluid/Thermal/Chemical Systems with Industrial Applications, ASME PVP Division Conf.*, 1–5 August 1999, Boston, USA, PVP. 1999. Vol. 397 (2). P. 143–154.
16. Menter F. R. Two-equation eddy viscosity turbulence models for engineering applications. *AIAA J.* 1994. Vol. 32. No. 8. P. 1598–1605. https://doi.org/10.2514/3.12149.
17. Русанов А. В., Пащенко Н. В. Аэродинамическое совершенствование цилиндра низкого давления паровой турбины мощностью 200 МВт. *Пробл. машиностроения.* 2009. Т. 12. No. 2. С. 7–15.

DOI: https://doi.org/10.15407/pmach2020.01.014

UDC 53:002

NONLOCAL ANISOTROPIC SHELL MODEL OF LINEAR VIBRATIONS OF MULTI-WALLED CARBON NANOTUBES

[1] Kostiantyn V. Avramov
kvavramov@gmail.com
ORCID: 0000-0002-8740-693X

[2] Balzhan N. Kabylbekova
balzhan.kbn@bk.ru
ORCID: 0000-0001-8461-8008

[2] Kazira K. Seitkazenova

[2] Darkhan S. Myrzaliyev

[2] Vladimir N. Pecherskiy

[1] A. Podgorny Institute of Mechanical Engineering Problems of NASU
2/10, Pozharsky str., Kharkiv, 61046, Ukraine

[2] M. Auezov South Kazakhstan State University
5, Tauke-khan Ave., Shymkent, 5160012, Kazakhstan

A simply-supported multi-walled carbon nanotube (MWCNT) is considered. Its vibrations will be studied in a cylindrical coordinate system. The elastic constants in Hooke's law depend on the CNT wall diameter, which is why each wall has its own elastic constants. CNT vibrations are described by the Sanders-Koiter shell theory. To derive partial differential equations (PDE) describing self-induced variations, a variational approach is used. The PDEs of vibrations are derived with respect to three projections of displacements. The model takes into account the Van der Waals forces between CNT walls. The three projections of displacements are expanded in basis functions. It was not possible to select the basis functions satisfying both geometric and natural boundary conditions. Therefore, selected are the basis functions that satisfy only geometric boundary conditions. To obtain a linear dynamic system with a finite number of degrees of freedom, the method of weighted residuals is used. To derive the basic relations of the method of weighted residuals, methods of variational calculus are used. The vibrational eigenfrequencies of single-walled (SW) CNTs are analyzed depending on the number of waves in the circumferential direction. With the number of waves in the circumferential direction from 2 to 4, the vibrational eigenfrequencies of CNTs are minimal. These numbers are smaller than those for the vibrational eigenfrequencies of engineering shells. Anisotropic models of tripple-walled (TW) CNTs were investigated. In their eigenforms, there is interaction between the basis functions and different numbers of waves in the longitudinal direction. This phenomenon was not observed in the isotropic CNT model. The appearance of such vibrations is a consequence of structural anisotropy.

Keywords: *nanotube, Sanders-Koiter shell model, Van der Waals forces, nonlocal elasticity.*

Introduction

CNT vibrations are extremely important for many nanomechanical devices, such as charge detectors, sensors, and devices for autoelectronic emission [1]. CNT vibrations are often observed during the processing and obtaining of nanocomposites. Wave processes in CNT-based nanodevices are studied in detail in articles [2, 3, 4]. CNT simulation approaches can be divided into two groups. The first group is a simulation based on molecular dynamics [5, 6], which requires huge computer resources. The second group is the construction of continuum models based on the mechanics of deformable solids. There are not many works that are devoted to the construction of shell models of CNT vibrations. In [7], a linear shell model is used to describe the vibrations of simply-supported CNTs. In [8], a model of linear CNT vibrations was obtained on the basis of the theory of Flygge shells with account taken of nonlocal elasticity. In studying the geometrically nonlinear dynamic deformation of CNTs, rod models are mainly used. In [9], continuous nonlinear beam models are used to model the nonlinear vibrations of MWCNTs. Nonlinear vibrations of the MWCNTs embedded in an elastic medium are considered in [10]. Nonlinear vibrations with large amplitudes of double-walled (DW) CNTs were studied by the finite element method in [11]. Forced vibrations of DWCNTs are considered in [12].

In this article, an anisotropic shell model of vibrations of a MWCNT is constructed. This model is based on the Sanders-Koiter shell theory. The interaction between the walls is described by Van der Waals forces. A system of PDEs is derived, describing CNT vibrations. To obtain a dynamic system with a finite number of degrees of freedom, the generalized Galerkin method is used. Properties of the linear vibrations of MWCNTs are investigated.

Statement of the Problem and Equations of Linear Vibrations

A MWCNT is considered, (Fig. 1). The number of CNT walls is equal. This MWCNT's vibrations will be studied in the cylindrical coordinate system (x, θ, z), Fig. 2. The figure shows one of CNT walls, which we will denote by the number i.

The individual deformations of CNT walls are interconnected due to Van der Waals forces. This deformation model is explained by the fact that van der Waals forces are much smaller than the covalent bonds of neighboring carbon atoms. The vibrations of each CNT wall will be studied on the shell-model basis [13]. We denote the three projections of the displacements of points of the middle surface of the ith wall by $u_i(x,\theta,t), v_i(x,\theta,t), w_i(x,\theta,t)$ (Fig. 2). Each CNT wall moves relative to the other walls. To describe wall elasticity, we use the nonlocal anisotropic Hooke's law [14, 15]. The elastic constants in Hooke's law depend on the CNT wall diameter [16, 17]. Therefore, each wall has its own elastic constants. Hooke's law for the ith wall has the following form:

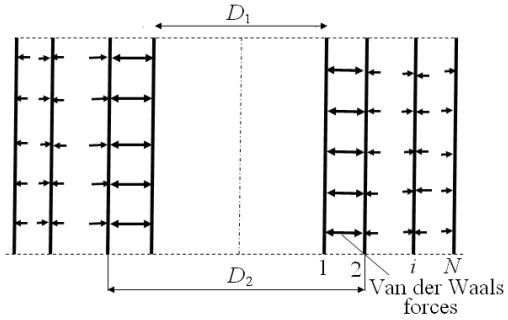

Fig.1. The outline of a MWCNT

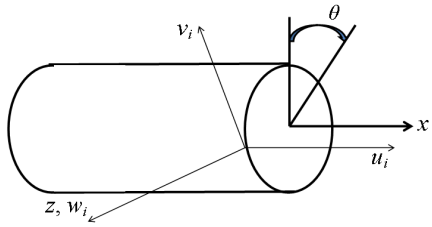

Fig. 2. Coordinates and unknowns of a ith wall of the CNT

$$\sigma_{xx}^{(i)} - \mu^2\nabla^2\sigma_{xx}^{(i)} = \frac{1}{h}\left(Y_{11}^{(i)}\varepsilon_{xx}^{(i)} + Y_{12}^{(i)}\varepsilon_{\theta\theta}^{(i)} + Y_{13}^{(i)}\gamma_{x\theta}^{(i)}\right),$$

$$\sigma_{\theta\theta}^{(i)} - \mu^2\nabla^2\sigma_{\theta\theta}^{(i)} = \frac{1}{h}\left(Y_{12}^{(i)}\varepsilon_{xx}^{(i)} + Y_{22}^{(i)}\varepsilon_{\theta\theta}^{(i)} + Y_{23}^{(i)}\gamma_{x\theta}^{(i)}\right),$$

$$\sigma_{x\theta}^{(i)} - \mu^2\nabla^2\sigma_{x\theta}^{(i)} = \frac{1}{h}\left(Y_{13}^{(i)}\varepsilon_{xx}^{(i)} + Y_{23}^{(i)}\varepsilon_{\theta\theta}^{(i)} + Y_{33}^{(i)}\gamma_{x\theta}^{(i)}\right), \quad (1)$$

where $\nabla^2(\,) = \dfrac{\partial^2(\,)}{\partial x^2} + \dfrac{\partial^2(\,)}{R_i^2\partial\theta^2}$; $\sigma_{xx}^{(i)}, \sigma_{\theta\theta}^{(i)}, \sigma_{x\theta}^{(i)}$ are the stress tensor elements; $\varepsilon_{xx}^{(i)}, \varepsilon_{\theta\theta}^{(i)}, \varepsilon_{x\theta}^{(i)}$ are the strain tensor elements; $\mu = e_0 a$ is the thin-film coefficient; R_i is the radius of the middle surface of the ith nanotube; h is the

thickness of each CNT wall; $Y_{jk}^{(i)}$ are the anisotropic elastic constants of the *i*th wall. As follows from [16, 17], the following relations hold: $Y_{13}^{(i)} = Y_{31}^{(i)} = -Y_{23}^{(i)} = -Y_{32}^{(i)}$.

The deformations $\varepsilon_{xx}^{(i)}, \varepsilon_{\theta\theta}^{(i)}, \varepsilon_{x\theta}^{(i)}$ of the *i*th wall at a distance z from the middle surface are described as follows:

$$\varepsilon_{xx}^{(i)} = \varepsilon_{x,0}^{(i)} + zk_x^{(i)}, \quad \varepsilon_{\theta\theta}^{(i)} = \varepsilon_{\theta,0}^{(i)} + zk_\theta^{(i)}, \quad \gamma_{x\theta}^{(i)} = \gamma_{x\theta,0}^{(i)} + zk_{x\theta}^{(i)},$$

where $\varepsilon_{x,0}^{(i)}, \varepsilon_{\theta,0}^{(i)}, \gamma_{x\theta,0}^{(i)}$ are the deformations of the middle surface of one of the CNT walls; $k_x^{(i)}, k_\theta^{(i)}, k_{X\theta}^{(i)}$ are the changes in curvature and torsion of the middle surface.

As was shown in [13], CNTs are well described by the Sanders-Koiter theory. Then the elements of the strain tensor, value $k_x^{(i)}, k_\theta^{(i)}, k_{x\theta}^{(i)}$, and projection of displacements satisfy the equations

$$\varepsilon_{x,0}^{(i)} = \frac{\partial u_i}{\partial x}, \quad \varepsilon_{\theta,0}^{(i)} = \frac{\partial v_i}{R_i \partial \theta} + \frac{w_i}{R_i}, \quad \gamma_{x\theta,0}^{(i)} = \frac{\partial u_i}{R_i \partial \theta} + \frac{\partial v_i}{\partial x},$$

$$k_x^{(i)} = \frac{-\partial^2 w_i}{\partial x^2}, \quad k_\theta^{(i)} = \frac{\partial v_i}{R_i^2 \partial \theta} - \frac{\partial^2 w_i}{R_i^2 \partial \theta^2}, \quad k_{x\theta}^{(i)} = -2\frac{\partial^2 w_i}{R_i \partial x \partial \theta} + \frac{1}{2R_i}\left(3\frac{\partial v_i}{\partial x} - \frac{\partial u_i}{R_i \partial \theta}\right). \tag{2}$$

The variation of the potential energy of the *i*th CNT wall is presented in the following form:

$$\delta \prod = \iint_A \left[N_{xx}^{(i)} \delta\varepsilon_{x,0}^{(i)} + N_{\theta\theta}^{(i)} \delta\varepsilon_{\theta,0}^{(i)} + N_{x\theta}^{(i)} \delta\gamma_{x\theta,0}^{(i)} + M_{xx}^{(i)} \delta k_x^{(i)} + M_{\theta\theta}^{(i)} \delta k_\theta^{(i)} + M_{x\theta}^{(i)} \delta k_{x\theta}^{(i)}\right] R_i dx d\theta \tag{3}$$

where A is the region of the middle surface of the shell; $N_{xx}^{(i)}, N_{\theta\theta}^{(i)}, N_{x\theta}^{(i)}, M_{xx}^{(i)}, M_{\theta\theta}^{(i)}, M_{x\theta}^{(i)}$ are the specific power factors and moments that are defined as follows:

$$N_{xx}^{(i)} = \int_{-0.5h}^{0.5h} \sigma_{xx}^{(i)} dz = \mu^2 \nabla^2 N_{xx}^{(i)} + Y_{11}^{(i)} \varepsilon_{x,0}^{(i)} + Y_{12}^{(i)} \varepsilon_{\theta,0}^{(i)} + Y_{13}^{(i)} \gamma_{x\theta,0}^{(i)},$$

$$N_{\theta\theta}^{(i)} = \int_{-0.5h}^{0.5h} \sigma_{\theta\theta}^{(i)} dz = \mu^2 \nabla^2 N_{\theta\theta}^{(i)} + Y_{12}^{(i)} \varepsilon_{x,0}^{(i)} + Y_{22}^{(i)} \varepsilon_{\theta,0}^{(i)} + Y_{23}^{(i)} \gamma_{x\theta,0}^{(i)},$$

$$N_{x\theta}^{(i)} = \int_{-0.5h}^{0.5h} \sigma_{x\theta}^{(i)} dz = \mu^2 \nabla^2 N_{x\theta}^{(i)} + Y_{13}^{(i)} \varepsilon_{x,0}^{(i)} + Y_{23}^{(i)} \varepsilon_{\theta,0}^{(i)} + Y_{33}^{(i)} \gamma_{x\theta,0}^{(i)},$$

$$M_{xx}^{(i)} = \int_{-0.5h}^{0.5h} z\sigma_{xx}^{(i)} dz = \mu^2 \nabla^2 M_{xx}^{(i)} + X_{11}^{(i)} k_x^{(i)} + X_{12}^{(i)} k_\theta^{(i)} + X_{13}^{(i)} k_{x\theta}^{(i)},$$

$$M_{\theta\theta}^{(i)} = \int_{-0.5h}^{0.5h} z\sigma_{\theta\theta}^{(i)} dz = \mu^2 \nabla^2 M_{\theta\theta}^{(i)} + X_{12}^{(i)} k_x^{(i)} + X_{22}^{(i)} k_\theta^{(i)} + X_{23}^{(i)} k_{x\theta}^{(i)},$$

$$M_{x\theta}^{(i)} = \int_{-0.5h}^{0.5h} z\sigma_{x\theta}^{(i)} dz = \mu^2 \nabla^2 M_{x\theta}^{(i)} + X_{13}^{(i)} k_x^{(i)} + X_{23}^{(i)} k_\theta^{(i)} + X_{33}^{(i)} k_{x\theta}^{(i)}, \tag{4}$$

where $X_{kj}^{(i)} = \dfrac{Y_{kj}^{(i)} h^2}{12}$.

We introduce (2) into equation (3) and perform integration by parts. Then, as a result, we obtain the following expression for the variation of potential energy:

$$\delta \prod = \iint_A \left[\Gamma_w^{(i)}(u_i, v_i, w_i)\delta w_i + \Gamma_v^{(i)}(u_i, v_i, w_i)\delta v_i + \Gamma_u^{(i)}(u_i, v_i, w_i)\delta u_i\right] R_i dx d\theta +$$

$$+ \int_0^{2\pi} \left[N_{xx}^{(i)} \delta u_i + B_v^{(i)}(u_i, v_i, w_i)\delta v_i + B_w^{(i)}(u_i, v_i, w_i)\delta w_i - M_{xx}^{(i)} \frac{\partial \delta w_i}{\partial x} \right]_0^L R_i d\theta, \tag{5}$$

where $[]_0^L = []_{x=0} - []_{x=L}$;

$$\Gamma_w^{(i)}(u_i,v_i,w_i)=\frac{-\partial}{\partial x}\left(N_{xx}^{(i)}\frac{\partial w_i}{\partial x}\right)+\frac{N_{\theta\theta}^{(i)}}{R_i}-\frac{\partial}{\partial\theta}\left[\frac{N_{\theta\theta}^{(i)}}{R_i}\left(\frac{\partial w_i}{R_i\partial\theta}-\frac{v_i}{R_i}\right)\right]-$$

$$-\frac{\partial}{\partial x}\left[N_{x\theta}^{(i)}\left(\frac{\partial w_i}{R_i\partial\theta}-\frac{v_i}{R_i}\right)\right]-\frac{\partial}{\partial\theta}\left[\frac{N_{x\theta}^{(i)}}{R_i}\frac{\partial w_i}{\partial x}\right]-\frac{\partial^2 M_{xx}^{(i)}}{\partial x^2}-\frac{\partial^2}{\partial\theta^2}\left(\frac{M_{\theta\theta}^{(i)}}{R_i^2}\right)-\frac{\partial^2}{\partial x\partial\theta}\left(\frac{2M_{x\theta}^{(i)}}{R_i}\right);$$

$$\Gamma_v^{(i)}(u_i,v_i,w_i)=\frac{-\partial}{\partial x}\left[\frac{N_{xx}^{(i)}}{4}\left(\frac{\partial v_i}{\partial x}-\frac{\partial u_i}{R_i\partial\theta}\right)\right]-\frac{\partial}{\partial\theta}\left(\frac{N_{\theta\theta}^{(i)}}{R_i}\right)-\frac{N_{\theta\theta}^{(i)}}{R_i^2}\left(\frac{\partial w_i}{\partial\theta}-v_i\right)+$$

$$+\frac{\partial}{\partial x}\left[\frac{N_{\theta\theta}^{(i)}}{4}\left(\frac{\partial u_i}{R_i\partial\theta}-\frac{\partial v_i}{\partial x}\right)\right]-\frac{\partial N_{x\theta}^{(i)}}{\partial x}-\frac{N_{x\theta}^{(i)}}{R_i}\frac{\partial w_i}{\partial x}-\frac{\partial}{\partial\theta}\left(\frac{M_{\theta\theta}^{(i)}}{R_i^2}\right)-\frac{3}{2R_i}\frac{\partial M_{x\theta}^{(i)}}{\partial x};$$

$$\Gamma_u^{(i)}(u_i,v_i,w_i)=\frac{-\partial N_{xx}^{(i)}}{\partial x}+\frac{\partial}{\partial\theta}\left[\frac{N_{xx}^{(i)}}{4R_i}\left(\frac{\partial v_i}{\partial x}-\frac{\partial u_i}{R_i\partial\theta}\right)\right]-\frac{\partial}{\partial\theta}\left[\frac{N_{\theta\theta}^{(i)}}{4R_i}\left(\frac{\partial u_i}{R_i\partial\theta}-\frac{\partial v_i}{\partial x}\right)\right]-\frac{\partial}{\partial\theta}\left(\frac{N_{x\theta}^{(i)}}{R_i}\right)+\frac{\partial}{\partial\theta}\left(\frac{M_{x\theta}^{(i)}}{2R_i^2}\right);$$

$$B_v^{(i)}(u_i,v_i,w_i)=\frac{N_{xx}^{(i)}+N_{\theta\theta}^{(i)}}{4}\left(\frac{\partial v_i}{\partial x}-\frac{\partial u_i}{R_i\partial\theta}\right)+N_{x\theta}^{(i)}+\frac{3}{2R_i}M_{x\theta}^{(i)};$$

$$B_w^{(i)}(u_i,v_i,w_i)=N_{xx}^{(i)}\frac{\partial w_i}{\partial x}+N_{x\theta}^{(i)}\left(\frac{\partial w_i}{R_i\partial\theta}-\frac{v_i}{R_i}\right)+\frac{\partial M_{xx}^{(i)}}{\partial x}+\frac{\partial}{\partial\theta}\left(\frac{2M_{x\theta}^{(i)}}{R_i}\right).$$

The variation of the kinetic energy of the *i*th CNT wall takes the following form:

$$\delta K=-\rho h\iint_A\left(\frac{\partial^2 u_i}{\partial t^2}\delta u_i+\frac{\partial^2 v_i}{\partial t^2}\delta v_i+\frac{\partial^2 w_i}{\partial t^2}\delta w_i\right)R_i dx d\theta, \tag{6}$$

where ρ is the material density. The virtual work of external surface forces is defined as follows:

$$\delta W=\iint_A\left(p_x^{(i)}\delta u_i+p_y^{(i)}\delta v_i+q_i\delta w_i\right)R_i dx d\theta, \tag{7}$$

where $p_x^{(i)}, p_y^{(i)}, q_i$ are the projections of external forces on the (x, θ, z) axes. To derive the CNT motion equations, we use the Hamilton principle

$$\int_{t_2}^{t_1}(\delta K-\delta\Pi+\delta W)dt=0 \tag{8}$$

where t_1, t_2 are some time values. We introduce (5, 6, 7) into equation (8) and obtain the following vibrational equations of the *i*th CNT wall:

$$\rho h\frac{\partial^2 u_i}{\partial t^2}-\frac{\partial N_{xx}^{(i)}}{\partial x}-\frac{\partial N_{x\theta}^{(i)}}{R_i\partial\theta}+\frac{\partial}{\partial\theta}\left[\frac{N_{xx}^{(i)}+N_{\theta\theta}^{(i)}}{4R_i}\left(\frac{\partial v_i}{\partial x}-\frac{\partial u_i}{R_i\partial\theta}\right)\right]+\frac{\partial M_{x\theta}^{(i)}}{2R_i^2\partial\theta}=p_x^{(i)}, \tag{9}$$

$$\rho h\frac{\partial^2 v_i}{\partial t^2}-\frac{\partial N_{\theta\theta}^{(i)}}{R_i\partial\theta}-\frac{\partial N_{x\theta}^{(i)}}{\partial x}-\frac{\partial}{\partial x}\left[\frac{N_{xx}^{(i)}+N_{\theta\theta}^{(i)}}{4}\left(\frac{\partial v_i}{\partial x}-\frac{\partial u_i}{R_i\partial\theta}\right)\right]-\frac{N_{\theta\theta}^{(i)}}{R_i^2}\left(\frac{\partial w_i}{\partial\theta}-v_i\right)-\frac{N_{x\theta}^{(i)}}{R_i}\frac{\partial w_i}{\partial x}-\frac{\partial M_{\theta\theta}^{(i)}}{R_i^2\partial\theta}-\frac{3\partial M_{x\theta}^{(i)}}{2R_i\partial x}=p_y^{(i)}, \tag{10}$$

$$\rho h\frac{\partial^2 w_i}{\partial t^2}-\frac{\partial}{\partial x}\left(N_{xx}^{(i)}\frac{\partial w_i}{\partial x}\right)+\frac{N_{\theta\theta}^{(i)}}{R_i}-\frac{\partial}{R_i^2\partial\theta}\left[N_{\theta\theta}^{(i)}\left(\frac{\partial w_i}{\partial\theta}-v_i\right)\right]-\frac{\partial}{R_i\partial x}\left[N_{x\theta}^{(i)}\left(\frac{\partial w_i}{\partial\theta}-v_i\right)\right]-\frac{\partial}{R_i\partial\theta}\left(N_{x\theta}^{(i)}\frac{\partial w_i}{\partial x}\right)-$$

$$-\frac{\partial^2 M_{xx}^{(i)}}{\partial x^2}-\frac{\partial^2 M_{\theta\theta}^{(i)}}{R_i^2\partial\theta^2}-\frac{2}{R_i}\frac{\partial^2 M_{x\theta}^{(i)}}{\partial\theta\,\partial x}=q_i. \tag{11}$$

We introduce relations (4) into (9, 10, 11) and obtain the following system of vibrational equations of the *i*th CNT wall

$$\rho h\Lambda\left(\frac{\partial^2 u_i}{\partial t^2}\right)-L_1^{(i)}\left(\frac{\partial u_i}{\partial x}\right)-L_2^{(i)}\left(\frac{\partial v_i}{R_i\partial\theta}+\frac{w_i}{R_i}\right)-L_3^{(i)}\left(\frac{\partial u_i}{R_i\partial\theta}+\frac{\partial v_i}{\partial x}\right)+L_4^{(i)}(u_i,v_i,w_i)=\Lambda\left(p_x^{(i)}\right)+F_u^{(i)}(u_i,v_i,w_i) \quad (12)$$

$$\rho h\Lambda\left(\frac{\partial^2 v_i}{\partial t^2}\right)-P_1^{(i)}\left(\frac{\partial u_i}{\partial x}\right)-P_2^{(i)}\left(\frac{\partial v_i}{R_i\partial\theta}+\frac{w_i}{R_i}\right)-P_3^{(i)}\left(\frac{\partial u_i}{R_i\partial\theta}+\frac{\partial v_i}{\partial x}\right)-P_4^{(i)}(u_i,v_i,w_i)=\Lambda\left(p_y^{(i)}\right)+F_v^{(i)}(u_i,v_i,w_i) \quad (13)$$

$$\rho h\Lambda\left(\frac{\partial^2 w_i}{\partial t^2}\right)+Q_1^{(i)}\left(\frac{\partial u_i}{\partial x}\right)+Q_2^{(i)}\left(\frac{\partial v_i}{R_i\partial\theta}+\frac{w_i}{R_i}\right)+Q_3^{(i)}\left(\frac{\partial u_i}{R_i\partial\theta}+\frac{\partial v_i}{\partial x}\right)-Q_4^{(i)}(u_i,v_i,w_i)=\Lambda(q_i)+F_w^{(i)}(u_i,v_i,w_i) \quad (14)$$

where $\Lambda, L_1^{(i)}, L_2^{(i)}, L_3^{(i)}, L_4^{(i)}, P_1^{(i)}, P_2^{(i)}, P_3^{(i)}, P_4^{(i)}, Q_1^{(i)}, Q_2^{(i)}, Q_3^{(i)}, Q_4^{(i)}$ are linear differential operators, which have the following form:

$$\Lambda(\cdot)=(\cdot)-\mu^2\nabla^2(\cdot), \qquad L_j^{(i)}(\cdot)=\frac{\partial}{\partial x}\left[Y_{1j}^{(i)}(\cdot)\right]+\frac{1}{R_i}\frac{\partial}{\partial\theta}\left[Y_{j3}^{(i)}(\cdot)\right],$$

$$P_j^{(i)}(\cdot)=\frac{\partial}{R_i\partial\theta}\left[Y_{2j}^{(i)}(\cdot)\right]+\frac{\partial}{\partial x}\left[Y_{j3}^{(i)}(\cdot)\right], \qquad Q_j^{(i)}(\cdot)=\frac{Y_{j2}^{(i)}}{R}(\cdot), \quad j=1,2,3,$$

$$L_4^{(i)}(u_i,v_i,w_i)=\frac{1}{2R_i^2}\frac{\partial}{\partial\theta}\left(X_{13}^{(i)}k_x^{(i)}+X_{23}^{(i)}k_\theta^{(i)}+X_{33}^{(i)}k_{x\theta}^{(i)}\right),$$

$$P_4^{(i)}(u_i,v_i,w_i)=\frac{\partial}{R_i^2\partial\theta}\left(X_{12}^{(i)}k_x^{(i)}+X_{22}^{(i)}k_\theta^{(i)}+X_{23}^{(i)}k_{x\theta}^{(i)}\right)+\frac{3}{2R_i}\frac{\partial}{\partial x}\left(X_{13}^{(i)}k_x^{(i)}+X_{23}^{(i)}k_\theta^{(i)}+X_{33}^{(i)}k_{x\theta}^{(i)}\right),$$

$$Q_4^{(i)}(u_i,v_i,w_i)=\frac{\partial^2}{\partial x^2}\left(X_{11}^{(i)}k_x^{(i)}+X_{12}^{(i)}k_\theta^{(i)}+X_{13}^{(i)}k_{x\theta}^{(i)}\right)+\frac{\partial^2}{R_i^2\partial\theta^2}\left(X_{12}^{(i)}k_x^{(i)}+X_{22}^{(i)}k_\theta^{(i)}+X_{23}^{(i)}k_{x\theta}^{(i)}\right)+$$

$$+\frac{2}{R_i}\frac{\partial^2}{\partial\theta\partial x}\left(X_{13}^{(i)}k_x^{(i)}+X_{23}^{(i)}k_\theta^{(i)}+X_{33}^{(i)}k_{x\theta}^{(i)}\right).$$

The CNT under consideration consists of the N walls that are interconnected by Van der Waals forces. Following [18], the projections of the van der Waals forces, q_i, acting on the ith CNT wall are determined as follows:

$$q_i=\sum_{j=1}^{N}c_{ij}\left(w_i-w_j\right) \quad (15)$$

where $c_{ij}=\frac{-\varepsilon R_j\pi}{a^4}\left\{\frac{1001\sigma^{12}}{3}E_{ij}^{(13)}-\frac{1120\sigma^6}{9}E_{ij}^{(7)}\right\}$, $E_{ij}^{(m)}=\left(R_i+R_j\right)^{-m}\int_0^{\pi/2}\frac{d\theta}{\left(1-K_{ij}\cos^2\theta\right)^{m/2}}$, $K_{ij}=\frac{4R_iR_j}{\left(R_j+R_i\right)^2}$, ε is the depth of the potential; σ is the parameter that determines the equilibrium; a is the C-C bond length; m is a positive integer.

Now we write a PDE system describing the geometrically nonlinear deformation of MWNTs. Equations of motion (12–14) should be applied to each of the embedded CNT walls. Then we write the equations of motion for a MWCNT as

$$\rho h\Lambda\left(\frac{\partial^2 u_i}{\partial t^2}\right)-L_1^{(i)}\left(\frac{\partial u_i}{\partial x}\right)-L_2^{(i)}\left(\frac{\partial v_i}{R_i\partial\theta}+\frac{w_i}{R_i}\right)-L_3^{(i)}\left(\frac{\partial u_i}{R_i\partial\theta}+\frac{\partial v_i}{\partial x}\right)+L_4^{(i)}(u_i,v_i,w_i)=F_u^{(i)}(u_i,v_i,w_i),$$

$$\rho h\Lambda\left(\frac{\partial^2 v_i}{\partial t^2}\right)-P_1^{(i)}\left(\frac{\partial u_i}{\partial x}\right)-P_2^{(i)}\left(\frac{\partial v_i}{R_i\partial\theta}+\frac{w_i}{R_i}\right)-P_3^{(i)}\left(\frac{\partial u_i}{R_i\partial\theta}+\frac{\partial v_i}{\partial x}\right)-P_4^{(i)}(u_i,v_i,w_i)=F_v^{(i)}(u_i,v_i,w_i),$$

$$\rho h\Lambda\left(\frac{\partial^2 w_i}{\partial t^2}\right)+Q_1^{(i)}\left(\frac{\partial u_i}{\partial x}\right)+Q_2^{(i)}\left(\frac{\partial v_i}{R_i\partial\theta}+\frac{w_i}{R_i}\right)+Q_3^{(i)}\left(\frac{\partial u_i}{R_i\partial\theta}+\frac{\partial v_i}{\partial x}\right)-Q_4^{(i)}(u_i,v_i,w_i)=\Lambda(q_i)+F_w^{(i)}(u_i,v_i,w_i)$$

$$i=1,\ \ldots,\ N. \quad (16)$$

We emphasize that the connection between the CNT walls during vibrations is realized through Van der Waals forces (15).

We write vibrational equations (16) with respect to dimensionless variables and parameters

$$\tilde{u}_i = \frac{u_i}{R_i}, \quad \tilde{v}_i = \frac{v_i}{R_i}, \quad \tilde{w}_i = \frac{w_i}{R_i}, \quad \eta = \frac{x}{L}, \quad \tau = \omega_0 t, \quad \delta_i = \frac{R_i}{R_1}; \quad \alpha_i = \frac{R_i}{L}; \quad i = 1,\ldots,N,$$

where $\omega_0^2 = \dfrac{Y_{11}^{(1)}}{hR_1^2\rho}$.

Relations (4) in dimensionless form will take the following form:

$$\tilde{\Lambda}\left(\tilde{N}_{xx}^{(i)}\right) = \tilde{Y}_{11}^{(i)}\tilde{\varepsilon}_{x,0}^{(i)} + \tilde{Y}_{12}^{(i)}\tilde{\varepsilon}_{\theta,0}^{(i)} + \tilde{Y}_{13}^{(i)}\tilde{\gamma}_{x\theta,0}^{(i)}, \qquad \tilde{\Lambda}\left(\tilde{N}_{\theta\theta}^{(i)}\right) = \tilde{Y}_{12}^{(i)}\tilde{\varepsilon}_{x,0}^{(i)} + \tilde{Y}_{22}^{(i)}\tilde{\varepsilon}_{\theta,0}^{(i)} + \tilde{Y}_{23}^{(i)}\tilde{\gamma}_{x\theta,0}^{(i)},$$

$$\tilde{\Lambda}\left(\tilde{N}_{x\theta}^{(i)}\right) = \tilde{Y}_{13}^{(i)}\tilde{\varepsilon}_{x,0}^{(i)} + \tilde{Y}_{23}^{(i)}\tilde{\varepsilon}_{\theta,0}^{(i)} + \tilde{Y}_{33}^{(i)}\tilde{\gamma}_{x\theta,0}^{(i)}, \qquad \tilde{\Lambda}\left(\tilde{M}_{xx}^{(i)}\right) = \tilde{X}_{11}^{(i)}\tilde{k}_x^{(i)} + \tilde{X}_{12}^{(i)}\tilde{k}_\theta^{(i)} + \tilde{X}_{13}^{(i)}\tilde{k}_{x\theta}^{(i)},$$

$$\tilde{\varepsilon}_{x,0}^{(i)} = \varepsilon_{x,0}^{(i)} = \alpha_i\frac{\partial\tilde{u}_i}{\partial\eta}, \qquad \tilde{\varepsilon}_{\theta,0}^{(i)} = \varepsilon_{\theta,0}^{(i)} = \frac{\partial\tilde{v}_i}{\partial\theta} + \tilde{w}_i, \qquad \tilde{\gamma}_{x\theta,0}^{(i)} = \gamma_{x\theta,0}^{(i)} = \frac{\partial\tilde{u}_i}{\partial\theta} + \alpha_i\frac{\partial\tilde{v}_i}{\partial\eta},$$

where $\left(\tilde{N}_{xx}^{(i)}, \tilde{N}_{\theta\theta}^{(i)}, \tilde{N}_{x\theta}^{(i)}\right) = \dfrac{1}{Y_{11}^{(1)}}\left(N_{xx}^{(i)}, N_{\theta\theta}^{(i)}, N_{x\theta}^{(i)}\right)$; $\tilde{\Lambda}(\cdot) = (\cdot) - \vartheta\tilde{\nabla}^2(\cdot)$; $\tilde{\nabla}^2(\cdot) = \dfrac{\partial^2(\cdot)}{\partial\eta^2} + \dfrac{1}{\alpha_i^2}\dfrac{\partial^2(\cdot)}{\partial\theta^2}$; $\vartheta = \dfrac{\mu^2}{L^2}$;

$$\tilde{Y}_{1j}^{(i)} = \frac{Y_{1j}^{(i)}}{Y_{11}^{(1)}}; \quad \tilde{Y}_{j3}^{(i)} = \frac{Y_{j3}^{(i)}}{Y_{11}^{(1)}}; \quad i = 1,\ldots,N; \quad j = 1,2,3; \qquad \tilde{Y}_{2j_1}^{(i)} = \frac{Y_{2j_1}^{(i)}}{Y_{11}^{(1)}}; \quad i = 1,\ldots,N; \quad j_1 = 2,3.$$

Dynamical system (16) in dimensionless form looks like this:

$$\tilde{\Lambda}\left(\delta_i\frac{\partial^2\tilde{w}_i}{\partial\tau^2}\right) + \tilde{Q}_1^{(i)}\left(\alpha_i\frac{\partial\tilde{u}_i}{\partial\eta}\right) + \tilde{Q}_2^{(i)}\left(\frac{\partial\tilde{v}_i}{\partial\theta} + \tilde{w}_i\right) + \tilde{Q}_3^{(i)}\left(\frac{\partial\tilde{u}_i}{\partial\theta} + \alpha_i\frac{\partial\tilde{v}_i}{\partial\eta}\right) - \tilde{Q}_4^{(i)}\left(\tilde{u}_i,\tilde{v}_i,\tilde{w}_i\right) = \tilde{\Lambda}\left(\tilde{q}_i\right) + \tilde{F}_w^{(i)}\left(\tilde{u}_i,\tilde{v}_i,\tilde{w}_i\right), \quad (17)$$

$$\tilde{\Lambda}\left(\delta_i\frac{\partial^2\tilde{u}_i}{\partial\tau^2}\right) - \tilde{L}_1^{(i)}\left(\alpha_i\frac{\partial\tilde{u}_i}{\partial\eta}\right) - \tilde{L}_2^{(i)}\left(\frac{\partial\tilde{v}_i}{\partial\theta} + \tilde{w}_i\right) - \tilde{L}_3^{(i)}\left(\frac{\partial\tilde{u}_i}{\partial\theta} + \alpha_i\frac{\partial\tilde{v}_i}{\partial\eta}\right) - \tilde{L}_4^{(i)}\left(\tilde{u}_i,\tilde{v}_i,\tilde{w}_i\right) = \tilde{F}_u^{(i)}\left(\tilde{u}_i,\tilde{v}_i,\tilde{w}_i\right), \quad (18)$$

$$\tilde{\Lambda}\left(\delta_i\frac{\partial^2\tilde{v}_i}{\partial\tau^2}\right) - \tilde{P}_1^{(i)}\left(\alpha_i\frac{\partial\tilde{u}_i}{\partial\eta}\right) - \tilde{P}_2^{(i)}\left(\frac{\partial\tilde{v}_i}{\partial\theta} + \tilde{w}_i\right) - \tilde{P}_3^{(i)}\left(\frac{\partial\tilde{u}_i}{\partial\theta} + \alpha_i\frac{\partial\tilde{v}_i}{\partial\eta}\right) - \tilde{P}_4^{(i)}\left(\tilde{u}_i,\tilde{v}_i,\tilde{w}_i\right) = \tilde{F}_v^{(i)}\left(\tilde{u}_i,\tilde{v}_i,\tilde{w}_i\right). \quad (19)$$

We represent these three PDEs in the following operator form:

$$G_1\left(\tilde{u}_i,\tilde{v}_i,\tilde{w}_i,\tilde{\Lambda}(\tilde{q}_i),\tilde{F}_w^{(i)}\right) = 0, \; G_2\left(\tilde{u}_i,\tilde{v}_i,\tilde{w}_i,\tilde{F}_u^{(i)}\right) = 0, \; G_3\left(\tilde{u}_i,\tilde{v}_i,\tilde{w}_i,\tilde{F}_v^{(i)}\right) = 0.$$

The dimensionless change in the curvature and torsion of the middle surface is defined as follows:

$$\tilde{k}_x^{(i)} = R_i k_x^{(i)} = -\alpha_i^2\frac{\partial^2\tilde{w}_i}{\partial\eta^2}, \; \tilde{k}_\theta^{(i)} = R_i k_\theta^{(i)} = \frac{\partial\tilde{v}_i}{\partial\theta} - \frac{\partial^2\tilde{w}_i}{\partial\theta^2}, \; \tilde{k}_{x\theta}^{(i)} = R_i k_{x\theta}^{(i)} = -2\alpha_i\frac{\partial^2\tilde{w}_i}{\partial\eta\partial\theta} + \frac{1}{2}\left(3\alpha_i\frac{\partial\tilde{v}_i}{\partial\eta} - \frac{\partial\tilde{u}_i}{\partial\theta}\right).$$

The dimensionless Van der Waals forces acting on CNT walls take the following form:

$$\tilde{q}_i = \sum_{j=1}^{N}\tilde{c}_{ij}\left(\delta_i\tilde{w}_i - \delta_j\tilde{w}_j\right),$$

where $\tilde{c}_{ij} = \tilde{\varepsilon}\delta_j\left[\dfrac{210\pi\tilde{\sigma}^6}{\left(\delta_i+\delta_j\right)^7}\tilde{E}_{ij}^{(7)} - \dfrac{9009\pi\tilde{\sigma}^{12}}{16\left(\delta_i+\delta_j\right)^{13}}\tilde{E}_{ij}^{(13)}\right]$; $\tilde{E}_{ij}^{(m)} = \displaystyle\int_0^{\pi/2}\frac{d\theta}{\left[1-\tilde{k}_{ij}\cos^2\theta\right]^{m/2}}$; $\tilde{\varepsilon} = \dfrac{16R_1^2\varepsilon}{27a^4Y_{11}^{(1)}}$; $\tilde{\sigma} = \dfrac{\sigma}{R_1}$;

$\tilde{k}_{ij} = \dfrac{4\delta_i\delta_j}{\left(\delta_i+\delta_j\right)^2}$.

Further, we consider a simply-supported MWCNT, which satisfies both the geometric boundary conditions

$$\tilde{w}_i\big|_{\eta=0} = \tilde{w}_i\big|_{\eta=1} = \tilde{v}_i\big|_{\eta=0} = \tilde{v}_i\big|_{\eta=1} = 0 \quad (20)$$

and natural boundary conditions

$$\tilde{M}_{xx}^{(i)}\big|_{\eta=0} = \tilde{M}_{xx}^{(i)}\big|_{\eta=1} = \tilde{N}_{xx}^{(i)}\big|_{\eta=0} = \tilde{N}_{xx}^{(i)}\big|_{\eta=1} = 0. \quad (21)$$

Equations of Motion with a Finite Number of Degrees of Freedom

To study vibrations, the Galerkin method is used [19]. Then it is necessary to satisfy both geometric (20) and natural boundary conditions (21). Taking into account relations (1), it is not possible to satisfy natural boundary conditions (21). Therefore, the generalized Galerkin method [19] is used, which is often called the method of weighted residuals [20]. We choose the expansions of displacements $\tilde{u}_i, \tilde{v}_i, \tilde{w}_i$, satisfying only geometric boundary conditions (20)

$$\tilde{u}_i = \sum_{m=1}^{J_1} \cos(m\pi\eta)\left[q_{i,m}^{(u,c)}(\tau)\cos(n\theta) + q_{i,m}^{(u,s)}(\tau)\sin(n\theta)\right],$$

$$v_i = \sum_{m=1}^{J_2} \sin(m\pi\eta)\left[q_{i,m}^{(v,c)}(\tau)\cos(n\theta) + q_{i,m}^{(v,s)}(\tau)\sin(n\theta)\right],$$

$$w_i = \sum_{m=1}^{J_3} \sin(m\pi\eta)\left[q_{i,m}^{(w,c)}(\tau)\cos(n\theta) + q_{i,m}^{(w,s)}(\tau)\sin(n\theta)\right], \tag{22}$$

where $q = \left[q^{(u,c)}, q^{(u,s)}, q^{(v,c)}, q^{(v,s)}, q^{(w,c)}, q^{(w,s)}\right]$ is the vector of generalized coordinates of dimension *N*.

In expansion (22), conjugate forms of vibrations must be present. If they are not taken into account in (22) and if such relations are introduced into PDEs (17–19), then conjugate forms will necessarily arise due to the presence of terms with $Y_{13}^{(i)}$ and $Y_{23}^{(i)}$ in Hooke's law (1).

In the variation of potential energy (5), taken into account are natural boundary conditions, which are represented by the second integral. These relations are used in the generalized Galerkin method [19]. We introduce relations (5, 6, 7) into (8). In the resulting equation, we turn to dimensionless variables and parameters. Then we get the following relation:

$$\iint_{A_i}\left\{G_1\left(\tilde{u}_i, \tilde{v}_i, \tilde{w}_i, \tilde{\Lambda}(\tilde{q}_i), \tilde{F}_w^{(i)}\right)\delta\tilde{u}_i + G_2\left(\tilde{u}_i, \tilde{v}_i, \tilde{w}_i, \tilde{F}_u^{(i)}\right)\delta\tilde{v}_i + G_3\left(\tilde{u}_i, \tilde{v}_i, \tilde{w}_i, \tilde{F}_v^{(i)}\right)\delta\tilde{w}_i\right\}d\eta\, d\theta +$$

$$+ \int_0^{2\pi}\left[\alpha_1\tilde{N}_{xx}^{(i)}\delta\tilde{u}_i - \alpha_1\alpha_i\tilde{M}_{xx}^{(i)}\frac{\partial\delta\tilde{w}_i}{\partial\eta}\right]_0^1 d\theta = 0, \tag{23}$$

where A_i is the dimensionless region of the middle surface of the *i*th CNT wall; $[\ ]_0^1 = [\ ]_{\eta=1} - [\ ]_{\eta=0}$.

Variational equation (23) yields the system of equations

$$\iint_{A_i} G_1\left(\tilde{u}_i, \tilde{v}_i, \tilde{w}_i, \tilde{\Lambda}(\tilde{q}_i), \tilde{F}_W^{(i)}\right)\sin(m_1\pi\eta)\begin{bmatrix}\cos(n\theta)\\ \sin(n\theta)\end{bmatrix}d\theta\, d\eta - \alpha_1\alpha_i m_1\pi\int_0^{2\pi}\left\{\tilde{M}_{xx}^{(i)}\cos(m_1\pi\eta)\begin{bmatrix}\cos(n\theta)\\ \sin(n\theta)\end{bmatrix}\right\}_0^1 d\theta = 0, \quad m_1 = 1,\ldots, J_3,$$

$$\iint_{A_i} G_2\left(\tilde{u}_i, \tilde{v}_i, \tilde{w}_i, \tilde{F}_u^{(i)}\right)\cos(m_1\pi\eta)\begin{bmatrix}\cos(n\theta)\\ \sin(n\theta)\end{bmatrix}d\theta\, d\eta + \alpha_1\int_0^{2\pi}\left\{\tilde{N}_{xx}^{(i)}\cos(m_1\pi\eta)\begin{bmatrix}\cos(n\theta)\\ \sin(n\theta)\end{bmatrix}\right\}_0^1 d\theta = 0, \quad m_1 = 1,\ldots, J_1,$$

$$\iint_{A_i} G_3\left(\tilde{u}_i, \tilde{v}_i, \tilde{w}_i, \tilde{F}_V^{(i)}\right)\sin(m_1\pi\eta)\begin{bmatrix}\cos(n\theta)\\ \sin(n\theta)\end{bmatrix}d\theta\, d\eta = 0, \quad m_1 = 1,\ldots, J_2 \tag{24}$$

Then, from relations (24), we obtain a linear dynamic system with a finite number of degrees of freedom, which has the following matrix form:

$$\mathbf{M}\ddot{\mathbf{q}} + \mathbf{K}\mathbf{q} + \mathbf{K}_\mathbf{B}\mathbf{q} = 0, \tag{25}$$

where **M** is the mass matrix; **Kq** is the product of the stiffness matrix and the vector of generalized coordinates, which describes the linear terms in equations (24). We emphasize that these terms are obtained by taking double integrals in (24). The linear terms $\mathbf{K_B q}$ are obtained by taking the single integrals included in (24). From system (25), an eigenvalue problem is easily derived for calculating the vibrational eigenfrequencies and modes.

System (25) describes the linear vibrations of CNTs with an arbitrary number of walls.

Numerical Vibrational Analysis of Single-walled CNTs

To verify the theory presented above, a numerical simulation of the eigenfrequencies of the linear vibrations of an isotropic CNT was carried out. A single-walled (SW) CNT with parameters [13] was considered: Eh=360 N/m, D=0.85 eV, ν=0.2, ρh=0.7718·10^{-6} kg/m^2, R_1=0.65 nm, where D is the cylindrical stiffness; Eh is the longitudinal stiffness; ν is Poisson's ratio; ρh is the mass per unit length. To calculate vibrational eigenfrequencies, the problem of eigenvalues, which is derived from system (25), is solved.

Table 1. The eigenfrequencies of an isotropic SWCNT

L/R_1	ω_1, Hz [1]	ω_1, Hz
0.5	8.189·10^{12}	8.193·10^{12}
1.0	4.968·10^{12}	4.972·10^{12}
5.0	1.042·10^{12}	1.043·10^{12}
10.0	3.288·10^{11}	3.290·10^{11}
50.0	1.468·10^{10}	1.469·10^{10}

The results of calculating vibrational eigenfrequencies are given in Table 1. The first column of the table shows the quantity L/R_1. The calculations were carried out for different CNT lengths. The second column presents the first eigenfrequency published in [13]. In this article, the vibrations of CNT continuum shell models were studied using the Sanders-Koiter theory. The third column presents the first eigenfrequency in Hz, obtained on the basis of the approach considered in Section 3. Thus, the first eigenfrequencies obtained by the two methods are close.

Eigenfrequencies of a simply-supported anisotropic SWCNT are studied. This SWCNT is described by the chiral indices, (n, m)=(15, 15). The SWCNT parameters were taken as follows:

$$K_\rho=742 \text{ N/m}, K_\theta=1.42 \text{ nN·nm}, r_0=0.142 \text{ nm}, \rho h=0.7718\cdot10^{-6} \text{ kg/m}^2, \quad (26)$$

where K_ρ, K_θ are constant forces associated with the stretching of the carbon-carbon bond and the angular curvature of bonds; r_0 is the carbon-carbon bond length. The parameters of Hooke's law (1) $Y_{ij}^{(1)}$ were calculated using the method proposed in [16, 17].

The results of calculating the eigenfrequencies of a simply-supported anisotropic SWCNT are presented in Fig. 3. Here, the eigenfrequencies for n=1 and n=2 expansions (22) are shown depending on the parameter $\pi R_1/L$. The solid line represents the eigenfrequencies obtained using the approach presented in Section 3. The diamonds in Fig. 3 show the eigenfrequencies published in [14]. The proximity of the eigenfrequencies obtained by the two different methods is the evidence that the eigenfrequencies calculated by us are correct. As the parameter $\pi R_1/L$ increases, the eigenfrequencies increase.

We study the dependence of the vibrational eigenfrequencies of a simply-supported anisotropic SWCNT with parameters (26) on the number of waves in the circumferential direction of n expansion (22). The results of this analysis are shown in Fig. 4. It shows the dependence of the eigenfrequencies ω_i on the number of waves in the circumferential direction. The calculations are presented for three parameter values $\pi R_1/L$: 1, 2.5; 4. For the parameter values $\pi R_1/L$=1; 2.5; 4, the minimum eigenfrequencies are observed at n=3; n=3; n=4, respectively.

As follows from [13], in isotropic CNT shell models, the minimum eigenfrequencies are observed at n=1 or n=2. In the shell considered here, the minimum eigenfrequencies are observed at somewhat larger n.

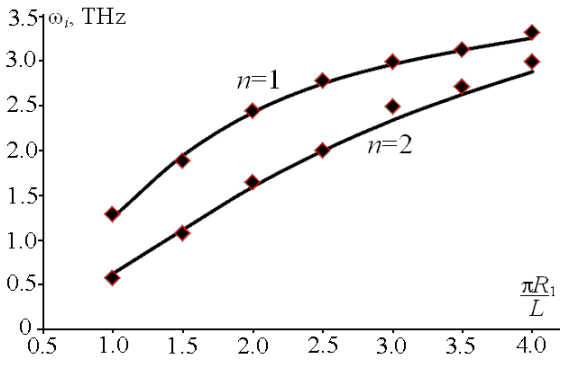

Fig. 3. The first eigenfrequencies at n=1 and n=2

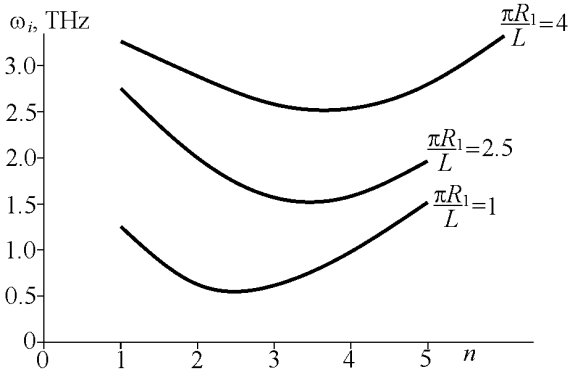

Fig. 4. The dependence of vibrational eigenfrequencies on the number of waves in the circumferential direction n

Numerical Vibrational Analysis of MWCNTs

Let us consider the results of calculating the eigenfrequencies of the linear vibrations of isotropic tripple-walled (TW) CNTs. The parameters of these CNTs are as follows: E=5.5 TPa; h=0.066 nm; ν=0.19; ρh=0.772·10^{-6} kg/m^2; R_1=5 nm; R_2=5.34 nm; R_3=5.68 nm; L=10R_3; a=0.142 nm; σ=0.3407 nm; ε=2.968 meV, where E is Young's modulus.

The results of calculating the eigenfrequencies of linear oscillations on the basis of an anisotropic model are shown in the second column of Table 2. The first two columns of the table show the number of waves in the circumferential direction n and the number m_g of the only nonzero harmonic in expansion (22), respectively. The results of calculating the vibrational eigenfrequencies of this isotropic TWCNT (see the third column of the table) were published in [21, 22]. So, the results of the calculations carried out by different methods are close.

Table 2. The eigenfrequencies of a TWCNT

n	m_g	ω_i, THz	ω_i, THz [15]
1	1	0.0360	0.0360
1	2	0.1161	0.1161
1	3	0.2069	0.2069
2	1	0.0139	0.0149
2	2	0.0467	0.0466
2	3	0.0944	0.0944

Table 3. The eigenfrequencies of an anisotropic TWCNT

n	m_g	ω_i, THz at J_1=J_2=J_3=3	ω_i, THz at J_1=J_2=J_3=4
1	1	0.21180	0.21180
	2	0.66310	0.66310
	3	1.14900	1.14900
2	1	0.57870	0.57870
	2	0.64830	0.64830
	3	0.83260	0.83250
3	1	1.06100	1.06100
	2	1.08173	1.08173
	3	1.13830	1.13830
4	1	1.53050	1.53050
	2	1.54750	1.54750
	3	1.58270	1.58270

We study the vibrations of the TWCNT with the chiral indices (5, 5); (10, 10); (15, 15), which was considered in [23]. The parameters of this CNT have the following values: R_1=0.339 nm; R_2=0.678 nm; R_3=1.016 nm; L=9R_3; a=0.142 nm; σ=0.3407 nm; ε=2.968 meV.

The matrix **Y** of Hooke's law (1) is calculated on the basis of the molecular approach presented in [16, 17]. For each CNT wall, the matrix ***Y*** has its own values. To calculate the eigenfrequencies, the approach proposed in Section 3 is used. The results of calculating the eigenfrequencies are presented in Table 3. The first column of the table shows the number of waves in the circumferential direction n in expansion (22). The second column shows the numbers of standing waves in the longitudinal direction m, which make a significant contribution to the decomposition of vibrational eigenmodes (22). The third column shows the first three eigenfrequencies obtained with the following parameters of expansion (22): J_1=J_2=J_3=3.

To analyze the convergence of the obtained eigenfrequencies [12, 13], they were calculated for a larger number of terms in expansion (22). The results of calculating the eigenfrequencies are shown in the fourth column of Table 3 at J_1=J_2=J_3=4. So, the calculation results presented in the third and fourth columns are close, which indicates their convergence.

As follows from the results given in Table 3, only one longitudinal half-wave with the number m_g prevails in its vibrational eigenmode (22). So, there is no interaction between the vibrational modes presented in expansion (22). This is due to the fact that the parameters included in Hooke's law (1) satisfy the equation $Y_{13}^{(i)} = Y_{23}^{(i)} = Y_{31}^{(i)} = Y_{32}^{(i)} = 0$. As follows from the further numerical analysis, at $Y_{13}^{(i)}, Y_{23}^{(i)}$ other than zero, there is an interaction between the vibrational modes in expansion (22).

Note that in all the eigenforms presented in Table 3, all three CNT walls vibrate in phase, i.e., they do not move in opposite radial directions.

The results of calculating the first three eigenfrequencies of a TWCNT are presented in Fig. 5. As follows from Fig. 5, a, with an increase in n starting from 1, the first eigenfrequency is constantly growing. The minimum value of the second and third eugenfrequencies is observed at n=2.

Consider the polychiral DWCNT whose electronic structure is discussed in [24]. Its chiral indices are: (9, 6) (15, 10). This CNT has the following wall radii: R_1=0.5119 nm; R_2=0.8532 nm; R_2–R_1=0.34 nm. The matrix **Y** of Hooke's law (1) was calculated on the basis of the molecular approach that was proposed in [16, 17]. The results of calculating the matrix ***Y*** for the two walls are presented in Table 4. The remaining CNT parameters were taken as follows: L=9R_2; a=0.142 nm; σ=0.3407 nm; ε=2.968 meV.

To calculate the eigenfrequencies, the approach presented in Section 3 was used. An analysis was made of the convergence of eigenfrequencies. Then, in expansions (22), the quantity J_1=J_2=J_3 changes. The influence of the quantity J_1 on the values of eigenfrequencies was investigated. The results of this analysis are given in Table 5. The first column of this table shows the number of terms in expansion (22).

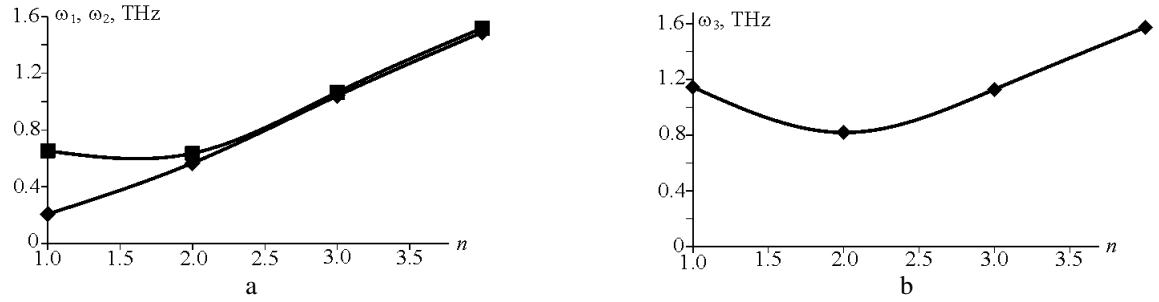

Fig. 5. The dependence of eigenfrequencies on the number of waves in the circumferential direction: a – the first and second eigenfrequencies; b – the third eigenfrequency

The second column shows the numbers of waves in the circumferential direction. The third, fourth, and fifth columns show the first three vibrational eigenfrequencies in THz. As follows from this table, at J_1=J_2=J_3=3 and 4 the eigen frequencies coincide, which indicates the convergence of results.

Now consider the properties of the eigenfrequencies obtained. The first eigenfrequency ω_1 increases with the number n of waves in the circumferential direction. The minimum value of the second and third eigenfrequencies is observed at n=2. With increasing n, the spectrum of the eigenfrequencies (ω_1, ω_2, ω_3) becomes tight. At n=1 and n=2 the spectrum of the eigenfrequencies is not tight, whereas at n=3 and n=4 it becomes tighter.

The results of the analysis of the eigenforms that correspond to the eigenfrequencies (Table 5) are systematized in Table 6. The first column of the table shows the number of waves in the circumferential direction n. In the second column, the numbers of vibrational eigenforms, $\overline{N}$, are presented. In the third one, the numbers of nonzero vibrational eigenmodes, m_g, that are present in expansion (22). With the number of waves in the circumferential direction n=1 and n=2, the vibrational eigenmodes (22) are represented as single-mode expansions. We emphasize that the number of a nonzero mode equals the number of the vibrational eigenmode. At n=3 and n=4 in the expansion of vibrational eigenmodes (22), several vibrational eigenmodes are present, which is shown in Table 6. Such an interaction between the vibrational modes is explained by the nonzero values of the parameters $Y_{13}^{(i)}, Y_{23}^{(i)}$ in Hooke's law (1).

Thus, if all the elements of the matrix **Y** of Hooke's law (1) are nonzero, then, in expansion (22), there is an interaction between the modes at linear vibrations.

Conclusion

This article provides a model of free CNT vibrations, which is expressed by a system of ordinary differential equations. To derive this dynamical system, we use a PDF system describing the deformation of MWCNTs and the method of weighted residuals. Thanks to the use of this method, the basis

Table 4. The anisotropic elastic constants of the polychiral DWCNT

Chiral indices	Y_{1x}	Y_{2x}	Y_{3x}	x
(9, 6)	368.150	60.240	-0.387	1
	60.240	368.150	0.387	2
	-0.387	0.387	152.000	3
(15,10)	369.090	59.300	-0.139	1
	59.300	369.090	0.139	2
	-0.139	0.139	154.190	3

Table 5. The convergence analysis of eigenfrequencies

J_1=J_2=J_3	n	ω_1, THz	ω_2, THz	ω_3, THz
2	1	0.2679	0.8396	–
3		0.2679	0.8396	1.4750
4		0.2679	0.8396	1.4750
2	2	0.4650	0.5874	–
3		0.4650	0.5874	0.8637
4		0.4650	0.5874	0.8637
2	3	1.1670	1.2010	–
3		1.1670	1.2010	1.2840
4		1.1670	1.2010	1.2840
3	4	1.8700	1.8950	1.9460
4		1.8700	1.8950	1.9460

Table 6. The modes of vibrations (22) involved in eigenforms

n	$\overline{N}$	m_g
1	1	1
	2	2
	3	3
2	1	1
	2	2
	3	3
3	1	1; 2
	2	1; 2; 3
	3	2; 3
4	1	1; 2
	2	1; 2; 3
	3	2; 3

functions over which the vibrations are expanded do not have to satisfy all the boundary conditions of the problem. It is these basis functions that are used in this paper. The mathematical model takes into account the CNT chirality, which is described by the anisotropic elastic constants of the model. Moreover, the nonlocal elasticity and Van der Waals forces between the CNT walls are taken into account in the model obtained.

The vibrational eigenfrequencies of SWCNTs are analyzed depending on the number of waves in the circumferential direction n. With the number of waves in the circumferential direction from 2 to 4, the minimum vibrational eigenfrequencies of CNTs are observed. These numbers are smaller than those for the vibrational eigenfrequencies of engineering shells.

References

1. Gibson, R. F., Ayorinde, E. O., & Wen, Y.-F. (2007). Vibrations of carbon nanotubes and their composites: A review. *Composites Sci. and Technology*, vol. 67, iss. 1, pp. 1–28. https://doi.org/10.1016/j.compscitech.2006.03.031.
2. Sirtori, C. (2002). Applied physics: Bridge for the terahertz gap. *Nature*, no. 417, pp. 132–133. https://doi.org/10.1038/417132b.
3. Jeon, T. & Kim, K. (2002). Terahertz conductivity of anisotropic single walled carbon nanotube films. *Appl. Physics Letters*, no. 80, pp. 3403–3405. https://doi.org/10.1063/1.1476713.
4. Yoon, J., Ru, C. Q., & Mioduchowski, A. (2003). Sound wave propagation in multiwall carbon nanotubes. *J. Appl. Physics*, no. 93, pp. 4801–4806. https://doi.org/10.1063/1.1559932.
5. Iijima, S., Brabec, C., Maiti, A., & Bernholc, J. (1996). Structural flexibility of carbon nanotubes. *J. Chemical Physics*, no. 104, pp. 2089–2092. https://doi.org/10.1063/1.470966.
6. Yakobson, B. I., Campbell, M. P., Brabec, C. J., & Bernholc, J. (1997). High strain rate fracture and C-chain unraveling in carbon nanotubes. *Computer Material Sci.*, vol. 8, iss. 4, pp. 241–248. https://doi.org/10.1016/S0927-0256(97)00047-5.
7. Wang, C. Y. & Zhang, L. C. (2008). An elastic shell model for characterizing single-walled carbon nanotubes. *Nanotechnology*, no. 19. 195704. https://doi.org/10.1088/0957-4484/19/19/195704.
8. Wang, Q. & Varadan, V. K. (2007). Application of nonlocal elastic shell theory in wave propagation analysis of carbon nanotubes. *Smart Material Structure*, no. 16, pp. 178–190. https://doi.org/10.1088/0964-1726/16/1/022.
9. Fu, Y. M., Hong, J. W., & Wang, X. Q. (2006). Analysis of nonlinear vibration for embedded carbon nanotubes. *J. Sound and Vibration*, vol. 296, iss. 4–5, pp. 746–756. https://doi.org/10.1016/j.jsv.2006.02.024.
10. Ansari, R. & Hemmatnezhad, M. (2001). Nonlinear vibrations of embedded multi-walled carbon nanotubes using a variational approach. *Mathematical and Computer Modeling*, vol. 53, iss. 5–6, pp. 927–938. https://doi.org/10.1016/j.mcm.2010.10.029.
11. Ansari, R. & Hemmatnezhad, M. (2012). Nonlinear finite element analysis for vibrations of double-walled carbon nanotubes. *Nonlinear Dynamics*, no. 67, pp. 373–383. https://doi.org/10.1007/s11071-011-9985-6.
12. Hajnayeb, A. & Khadem, S. E. (2012). Analysis of nonlinear vibrations of double-walled carbon nanotubes conveying fluid. *J. Sound and Vibration*, vol. 331, iss. 10, pp. 2443–2456. https://doi.org/10.1016/j.jsv.2012.01.008.
13. Avramov, K. V. (2018). Nonlinear vibrations characteristics of single-walled carbon nanotubes via nonlocal elasticity. *Intern. J. Nonlinear Mech.*, vol. 107, pp. 149–160. https://doi.org/10.1016/j.ijnonlinmec.2018.08.017.
14. Fazelzadeh, S. A. & Ghavanloo, E. (2012). Nonlocal anisotropic elastic shell model for vibrations of single-walled carbon nanotubes with arbitrary chirality. *Composite Structures*, vol. 94, iss. 3, pp. 1016–1022. https://doi.org/10.1016/j.compstruct.2011.10.014.
15. Ghavanloo, E. & Fazelzadeh, S. A. (2012). Vibration characteristics of single-walled carbon nanotubes based on an anisotropic elastic shell model including chirality effect. *Appl. Math. Modelling*, vol. 36, iss. 10, pp. 4988–5000. https://doi.org/10.1016/j.apm.2011.12.036.
16. Chang, T. (2010). A molecular based anisotropic shell model for single-walled carbon nanotubes. *J. Mech. and Physics Solids*, vol. 58, iss. 9, pp. 1422–1433. https://doi.org/10.1016/j.jmps.2010.05.004.
17. Chang, T., Geng, J., & Guo, X. (2006). Prediction of chirality- and size-dependent elastic properties of single-walled carbon nanotubes via a molecular mechanics model. *Proc. Royal Society A*, vol. 462, iss. 2072, pp. 2523–2540. https://doi.org/10.1098/rspa.2006.1682.
18. He, X. Q., Kitipornchai, S., Wang, C. M., Xiang, Y., & Zhou, Q. (2010). A nonlinear Van Der Waals force model for multiwalled carbon nanotubes modeled by a nested system of cylindrical shells. *ASME J. Appl. Mech.*, vol.77, iss. 6, 061006 (6 p.). https://doi.org/10.1115/1.4001859.
19. Washizu, K. (1975). Variational methods in elasticity and plasticity. Oxford, United Kingdom: Pergamon Press, 420 p.
20. Zienkiewicz, O. (1983). Finite elements and approximation. New York: John Wiley & Sons, 350 p.
21. He, X. Q., Kitipornchai, S., & Liew, K. M. (2005). Buckling analysis of multi-walled carbon nanotubes: A continuum model accounting for Van der Waals interaction. *J Mech. Phys. Solids*, vol. 53, iss. 2, pp. 303–326. https://doi.org/10.1016/j.jmps.2004.08.003.

22. Strozzi, M. & Pellicano, F. (2017). Linear vibrations of triple-walled carbon nanotubes. *Mathematics and Mechanics of Solids*, vol. 23, iss. 11, pp. 1456–1481. https://doi.org/10.1177/1081286517727331.
23. Liew, K. M., He, X. Q., & Wong, C. H. (2004). On the study of elastic and plastic properties of multi-walled carbon nanotubes under axial tension using molecular dynamics simulation. *Acta Materialia*, vol. 52, iss. 9, pp. 2521–2527. https://doi.org/10.1016/j.actamat.2004.01.043.
24. Lambin, Ph., Meunier, V., & Rubio, A. (2000). Electronic structure of polychiral carbon nanotubes. *Physical review B*, vol. 62, iss. 8, pp. 5129–5135. https://doi.org/10.1103/PhysRevB.62.5129.

Received 13 February 2020

Нелокальна анізотропна оболонкова модель лінійних коливань багатостінних вуглецевих нанотрубок

[1] К. В. Аврамов, [2] Б. Н. Кабилбекова, [2] К. К. Сейтказенова, [2] Д. С. Мирзалієв, [2] В. М. Печерський

[1] Інститут проблем машинобудування ім. А. М. Підгорного НАН України,
61046, Україна, м. Харків, вул. Пожарського, 2/10

[2] Південно-Казахстанський державний університет імені Мухтара Ауезова
160012, Казахстан, м. Шимкент, пр. Тауке-хана, 5

Розглядається багатостінна шарнірно-обперта вуглецева нанотрубка. Її коливання будуть вивчатися в циліндричній системі координат. Пружні сталі в законі Гука залежать від діаметра стінки вуглецевої нанотрубки. Тому кожна стінка має свої пружні сталі. Коливання стінок нанотрубок описуються оболонковою теорією Сандерса-Коітера. Для виведення рівнянь в частинних похідних, що описують автоколивання, застосовується варіаційний підхід. Рівняння коливань в частинних похідних виводяться щодо трьох проекцій переміщень. У моделі враховуються сили Ван-дер-Ваальса між стінками нанотрубки. Три проекції переміщень розкладаються за базисними функціями. Вибрати базисні функції, що задовольняють одночасно геометричні і природні граничні умови, не вдалося. Тому вибираються базисні функції, що задовольняють тільки геометричні граничні умови. Для одержання лінійної динамічної системи зі скінченним числом ступенів свободи застосовується метод зважених нев'язок. Для виведення основних співвідношень методу зважених нев'язок застосовуються методи варіаційного числення. Проведено аналіз власних частот коливань одностінних вуглецевих нанотрубок в залежності від числа хвиль в обводовому напрямку. За числа хвиль в обводовому напрямку від 2 до 4 спостерігаються мінімальні власні частоти коливань нанотрубок. Ці числа менші, ніж для власних частот коливань машинобудівних оболонок. Досліджувалися трьохстінні анізотропні моделі нанотрубок. У власних формах спостерігається взаємодія між базисними функціями з різним числом хвиль в поздовжньому напрямку. Цього явища не спостерігалося в ізотропній моделі нанотрубки. Поява таких коливань є наслідком анізотропії конструкції.

***Ключові слова**: нанотрубка, оболонкова теорія Сандерса–Коітера, сили Ван-дер-Ваальса, нелокальна пружність.*

Література

1. Gibson R. F., Ayorinde E. O., Wen Y.-F. Vibrations of carbon nanotubes and their composites: A review. *Composites Sci. and Technology*. 2007. Vol. 67. Iss. 1. P. 1–28. https://doi.org/10.1016/j.compscitech.2006.03.031.
2. Sirtori C. Applied physics: Bridge for the terahertz gap. *Nature.* 2002. No. 417. P. 132–133. https://doi.org/10.1038/417132b.
3. Jeon T., Kim K. Terahertz conductivity of anisotropic single walled carbon nanotube films. *Appl. Physics Letters.* 2002. No. 80. P. 3403–3405. https://doi.org/10.1063/1.1476713.
4. Yoon J., Ru C. Q., Mioduchowski A. Sound wave propagation in multiwall carbon nanotubes. *J. Appl. Physics*. 2003. No. 93. P. 4801–4806. https://doi.org/10.1063/1.1559932.
5. Iijima S., Brabec C., Maiti A., Bernholc J. Structural flexibility of carbon nanotubes. *J. Chemical Physics*. 1996. No. 104. P. 2089–2092. https://doi.org/10.1063/1.470966.
6. Yakobson B. I., Campbell M. P., Brabec C. J., Bernholc J. High strain rate fracture and C-chain unraveling in carbon nanotubes. *Computer Material Sci*. 1997. Vol. 8. Iss. 4. P. 241–248. https://doi.org/10.1016/S0927-0256(97)00047-5.
7. Wang C. Y., Zhang L. C. An elastic shell model for characterizing single-walled carbon nanotubes. *Nanotechnology.* 2008. No. 19. 195704. https://doi.org/10.1088/0957-4484/19/19/195704.

8. Wang Q., Varadan V. K. Application of nonlocal elastic shell theory in wave propagation analysis of carbon nanotubes. *Smart Material Structure*. 2007. No. 16. P. 178–190. https://doi.org/10.1088/0964-1726/16/1/022.
9. Fu Y. M., Hong J. W., Wang X. Q. Analysis of nonlinear vibration for embedded carbon nanotubes. *J. Sound and Vibration*. 2006. Vol. 296. Iss. 4–5. P. 746–756. https://doi.org/10.1016/j.jsv.2006.02.024.
10. Ansari R., Hemmatnezhad M. Nonlinear vibrations of embedded multi-walled carbon nanotubes using a variational approach. *Mathematical and Computer Modeling*. 2011. Vol. 53. Iss. 5–6. P. 927–938. https://doi.org/10.1016/j.mcm.2010.10.029.
11. Ansari R., Hemmatnezhad M. Nonlinear finite element analysis for vibrations of double-walled carbon nanotubes. *Nonlinear Dynamics.* 2012. No. 67. P. 373–383. https://doi.org/10.1007/s11071-011-9985-6.
12. Hajnayeb A., Khadem S. E. Analysis of nonlinear vibrations of double-walled carbon nanotubes conveying fluid. *J. Sound and Vibration*. 2012. Vol. 331. Iss. 10. P. 2443–2456. https://doi.org/10.1016/j.jsv.2012.01.008.
13. Avramov K. V. Nonlinear vibrations characteristics of single-walled carbon nanotubes via nonlocal elasticity. *Intern. J. Nonlinear Mech*. 2018. Vol. 107. P. 149–160. https://doi.org/10.1016/j.ijnonlinmec.2018.08.017.
14. Fazelzadeh S. A., Ghavanloo E. Nonlocal anisotropic elastic shell model for vibrations of single-walled carbon nanotubes with arbitrary chirality. *Composite Structures.* 2012. Vol. 94. Iss. 3. P. 1016–1022. https://doi.org/10.1016/j.compstruct.2011.10.014.
15. Ghavanloo E., Fazelzadeh S. A. Vibration characteristics of single-walled carbon nanotubes based on an anisotropic elastic shell model including chirality effect. *Appl. Math. Modelling*. 2012. Vol. 36. Iss. 10. P. 4988–5000. https://doi.org/10.1016/j.apm.2011.12.036.
16. Chang T. A molecular based anisotropic shell model for single-walled carbon nanotubes. *J. Mech. and Physics Solids*. 2010. Vol. 58. Iss. 9. P. 1422–1433. https://doi.org/10.1016/j.jmps.2010.05.004.
17. Chang T., Geng J., Guo X. Prediction of chirality- and size-dependent elastic properties of single-walled carbon nanotubes via a molecular mechanics model. *Proc. Royal Society A*. 2006. Vol. 462. Iss. 2072. P. 2523–2540. https://doi.org/10.1098/rspa.2006.1682.
18. He X. Q., Kitipornchai S., Wang C. M., Xiang Y., Zhou Q. A nonlinear Van Der Waals force model for multi-walled carbon nanotubes modeled by a nested system of cylindrical shells. *ASME J. Appl. Mech.* 2010. Vol.77. Iss. 6. 061006 (6 p.). https://doi.org/10.1115/1.4001859.
19. Washizu K. Variational methods in elasticity and plasticity. Oxford, United Kingdom: Pergamon Press, 1975. 420 p.
20. Zienkiewicz O., et al. Finite elements and approximation. New York: John Wiley & Sons, 1983. 350 p.
21. He X. Q., Kitipornchai S., Liew K. M. Buckling analysis of multi-walled carbon nanotubes: A continuum model accounting for Van der Waals interaction. *J Mech. Phys. Solids.* 2005. Vol. 53. Iss. 2. P. 303–326. https://doi.org/10.1016/j.jmps.2004.08.003.
22. Strozzi M., Pellicano F. Linear vibrations of triple-walled carbon nanotubes. *Mathematics and Mechanics of Solids*. 2017. Vol. 23. Iss. 11. P. 1456–1481. https://doi.org/10.1177/1081286517727331.
23. Liew K. M., He X. Q., Wong C. H. On the study of elastic and plastic properties of multi-walled carbon nanotubes under axial tension using molecular dynamics simulation. *Acta Materialia*. 2004. Vol. 52. Iss. 9. P. 2521–2527. https://doi.org/10.1016/j.actamat.2004.01.043.
24. Lambin Ph., Meunier V., Rubio A. Electronic structure of polychiral carbon nanotubes. *Physical review B*. 2000. Vol. 62. Iss. 8. P. 5129–5135. https://doi.org/10.1103/PhysRevB.62.5129.